

# Smearing of the phase transition in Ising systems with planar defects

Thomas Vojta

Department of Physics, University of Missouri-Rolla, Rolla, MO 65409, USA

**Abstract.** We show that phase transitions in Ising systems with planar defects, i.e., disorder perfectly correlated in two dimensions are destroyed by smearing. This is caused by effects similar to but stronger than the Griffiths phenomena: Exponentially rare spatial regions can develop true static long-range order even when the bulk system is still in its disordered phase. Close to the smeared transition, the order parameter is very inhomogeneous in space, with the thermodynamic (average) order parameter depending exponentially on temperature. We determine the behavior using extremal statistics, and we illustrate the results by computer simulations.

## 1. Introduction

Phase transitions in random systems remain one of the important and only partially solved problems in statistical physics. Originally, it was thought that even weak disorder destroys any critical point because the disordered system divides itself up into spatial regions which undergo the transition at different temperatures, leading to a smeared transition in which there would be no sharp singularities in thermodynamic quantities (see [1] and references therein). However, it was soon found that classical continuous phase transitions are generically sharp in the presence of weak, short-range correlated disorder. If a clean critical fixed point (FP) fulfills the Harris criterion [2]

$2-\nu > d$ , where  $\nu$  is the correlation length exponent and  $d$  is the spatial dimensionality, the disorder decreases under coarse graining. The system becomes asymptotically homogeneous at large length scales. Thus, the clean critical point is perturbatively stable against disorder, and the critical behavior of the random system is identical to that of the corresponding clean system. Macroscopic observables are self-averaging at the critical point, i.e., the relative width of their probability distributions goes to zero in the thermodynamic limit [3,4].

Even if the Harris criterion is violated, the transition will generically remain sharp, but the critical behavior will be different from that of the clean system. Depending on the fate of the disorder under coarse graining it can either be of finite or of infinite disorder type. In the first case the system remains inhomogeneous at all length scales with the relative strength of the inhomogeneities approaching a finite value for large length scales. These transitions are controlled by renormalization group (RG) fixed points with finite disorder. Macroscopic observables are not self-averaging, the relative width of their probability distributions approaches a size-independent constant [3,4]. Examples of critical points in this class include the dilute three-dimensional Ising model or classical spin glasses. The second case occurs when the relative magnitude of

the inhomogeneities increase without limit under coarse graining. The corresponding fixed points are called infinite-disorder fixed points. Here, the probability distributions of microscopic variables become very broad (on a logarithmic scale) with the width increasing with system size. This can lead to activated rather than the usual power-law scaling at the critical point. A famous classical example of an infinite-disorder critical point occurs in the McCoy-Wu model [5].

In recent years, another aspect of phase transitions in disordered systems, the Griffiths phenomena, has regained a lot of attention. Griffiths phenomena are non-perturbative effects of rare disorder fluctuations in the vicinity of a phase transition. They can be understood as follows: Disorder in general decreases the critical temperature  $T_c$  from its clean value  $T_c^0$ . In the temperature region  $T_c < T < T_c^0$  the system does not display global order. However, in an infinite system one will find arbitrarily large regions that are devoid of impurities with a small but non-zero probability. These rare regions or 'Griffiths islands' are locally in the ordered phase while the bulk system is still in the disordered phase. Their fluctuations are very slow because flipping them requires changing the order parameter in a large volume. Griffiths [6] was the first to show that this leads to a non-analytic free energy everywhere in the region  $T_c < T < T_c^0$ , which is now known as the Griffiths phase [7] or the Griffiths region. In generic classical systems, the contribution of the Griffiths singularities to thermodynamic (equilibrium) observables is very weak since the singularity in the free energy is only an essential one [6,8]. In contrast, the consequences for the dynamics are much more severe with the rare regions dominating the behavior for long times. In the Griffiths region, the spin autocorrelation function  $C(t)$  decays very slowly with time  $t$ , like  $\ln C(t) \sim -(\ln t)^{d/(d-1)}$  for Ising systems [7,9,12], and like  $\ln C(t) \sim -t^{-2}$  for Heisenberg systems [11,13]. More recently, these results have been confirmed by rigorous calculations for the equilibrium [14,15] and dynamic [16] properties of disordered Ising models.

In many real systems, the disorder is not generated by point-like defects but by dislocations or disordered layers or grain boundaries. Often, extended impurities in a  $d$ -dimensional system can be modeled by disorder perfectly correlated in  $d_c = 1$  or 2 dimensions but uncorrelated in the remaining  $d_\perp = d - d_c$  dimensions. While it is generally accepted that long-range disorder correlations increase the effects of the impurities, their influence on the phase transition has been controversial. Early RG work [17] based on a single expansion in  $d = 4 - \epsilon$  did not produce a critical fixed point. This was interpreted as a smeared transition or a first order one [18,19]. However, an additional expansion in the number  $d_c$  of correlated dimensions [20-22] cured this problem and gave rise to critical fixed points with conventional power-law scaling. Further support for the sharp transition scenario came from Monte-Carlo simulations of a 3D Ising model with planar defects [23]. All the perturbative RG studies miss, however, the effects of rare regions and Griffiths phenomena. These effects have been studied in detail in the already mentioned McCoy-Wu model [5], a disordered 2D Ising model in which the disorder is perfectly correlated in one dimension and uncorrelated in the other. The transition in this model was originally thought to be smeared. It was later found that it is sharp but of infinite-disorder type [24,25]. Similar behavior has been found in several random quantum systems which are related to classical systems with linear defects [26-31]. Based on these results it was believed for a long time that phase transitions generically remain sharp even in the presence of extended disorder.

In this paper we show, however, that this belief is not generally true. Specifically, we show that for Ising order parameter symmetry, planar defects destroy the sharp

continuous phase transition via effects which are similar to but stronger than the usual Griffiths phenomena: In systems with planar defects true static long-range order can develop on isolated rare regions. As a result, the order parameter is very inhomogeneous in space close to the smeared transition, and the thermodynamic order parameter depends exponentially on temperature. We also show that this disorder-induced smearing generically occurs in an entire class of transitions in systems with extended disorder. The paper is organized as follows. In Sec. 2, the model is introduced, and the mechanism for the smearing of the transition is explained. In Sec. 3 we use Lifshitz tail arguments to determine the behavior in the 'tail' of the rounded transition, i.e., for a very low concentration of ordered islands. Section 4 is devoted to a numerical study of a three-dimensional infinite-range Ising model which illustrates the smearing of the phase transition. Finally, in Sec. 5 we discuss the generality of the disorder-induced smearing, the relation to Griffiths phenomena, favorable conditions for observing the smearing, and the influence of the order parameter symmetry.

## 2. Rare regions, inhomogeneous order, and smearing

For definiteness we consider a  $d$ -dimensional  $\phi^4$  theory with random  $-T_c$  type disorder completely correlated in the  $d_c = 2$  directions  $x_1$  and  $x_2$  but uncorrelated in the remaining  $d_\perp = d - d_c$  directions  $x_3; \dots; x_d$ . The action is given by

$$S = \int d^d r \left( \frac{1}{2} (\nabla \phi)^2 + t \phi^2 + \frac{u}{4} \phi^4 \right) + \int d^2 r_\perp \int d^{d_\perp} r_\parallel \left( \frac{1}{2} (\nabla_\perp \phi)^2 + t_\perp \phi^2 + \frac{u}{4} \phi^4 \right) : \quad (1)$$

Here  $\phi(r)$  is a scalar field,  $t$  is the dimensionless distance from the clean critical point and  $t_\perp$  introduces the quenched disorder.  $r_\perp$  is the projection of  $r$  on the uncorrelated directions  $x_3; \dots; x_d$ . We consider two different types of disorder. In the first type, Poisson (or dilution) disorder,  $t_\perp$  is given by

$$t_\perp(r_\perp) = \sum_i V(r_\perp - r_\perp(i)) \quad (2)$$

where  $r_\perp(i)$  are the random positions of planar impurities of spatial density  $c$ , and  $V(r_\perp)$  is a non-negative short-ranged impurity potential. The second type of disorder is a Gaussian distribution with zero mean and a correlation function

$$\langle t_\perp(r_\perp) t_\perp(r'_\perp) \rangle = \delta^2(r_\perp - r'_\perp) : \quad (3)$$

Now consider the effects of rare disorder fluctuations in this system: Analogous to the Griffiths phenomena, there is a small but finite probability for finding large spatial regions in  $r_\perp$  direction which are more strongly coupled than the bulk system. For Poisson disorder, these are regions devoid of impurities while for Gaussian disorder it would be regions with a negative average  $\langle t_\perp(r_\perp) \rangle$ . These rare regions can be locally in the ordered phase, even if the bulk system is still in the disordered phase. For Poisson disorder which fulfills  $\langle t_\perp(r_\perp) \rangle > 0$  this starts to happen right below the clean transition, i.e., for  $t < 0$  [32] while for the unbounded Gaussian disorder, locally ordered rare regions exist for all  $t$ . Since the defects in our system are planar, the rare regions are finite in the  $x_1$  and  $x_2$  directions but infinite in the remaining directions. This is a crucial difference to systems with uncorrelated disorder, where the rare regions are finite objects (see Sec. 5). In our system, each rare region is therefore equivalent to a two-dimensional Ising system and can undergo a real phase transition independently of the rest of the system. Thus, for planar defects, those rare regions which are in the

ordered phase will develop a non-zero static order parameter which can be aligned by an infinitesimally small interaction or an infinitesimally small field.

The resulting phase transition is very different from conventional continuous phase transitions, be it transitions controlled by clean or finite-disorder or even in finite-randomness fixed points. In all of those cases, which represent "sharp" phase transitions, a non-zero order parameter develops as a collective effect of the entire system, accompanied by a diverging correlation length in all directions. In contrast, in a system with planar defects, the order parameter develops very inhomogeneously in space with different parts of the system (i.e., different  $r_\perp$  regions) ordering independently at different  $t$ . Correspondingly, the correlation length in  $r_\perp$  direction remains finite for all temperatures. This defines a smeared transition. We thus conclude that planar defects lead to a smearing of the phase transition.

Above, we have defined a smeared continuous phase transition via the behavior of correlation length. We now characterize it via the behavior of the free energy density or other global thermodynamic variables. Two qualitatively different cases of smeared transitions must be distinguished. If the disorder distribution is unbounded in the sense that it permits regions with a local  $T_c = 1$  (system (1) with Gaussian disorder falls into this class), the total (average) order parameter is non-zero for all temperatures, and the free energy density is analytic. In contrast, if the disorder distribution is bounded, there is a true paramagnetic phase with zero order parameter at high temperatures. At some temperature  $T_0$ , a non-zero order parameter starts to develop on rare spatial regions, accompanied by an essential singularity in the free energy density (which stems from the probability for finding a rare region). This singularity is weaker than the power-law singularities at the sharp transitions mentioned above. The model (1) with Poisson disorder falls into this second class, with  $T_0$  being identical to the critical temperature of the pure system.

### 3. Lifshitz tail arguments

In this section we use extremal statistics to derive the leading thermodynamic behavior in the "tail" of the smeared transition, i.e., in the parameter region where a few islands have developed static order but their density is so small that they can be treated as independent. The approach is similar to that of Lifshitz [33] and others for the description of the tails in the electronic density of states. We first consider the Poisson type of disorder and later describe the differences for Gaussian disorder.

#### 3.1. Poisson disorder

The probability  $w$  of finding a large region of linear size  $L_R$  (in  $r_\perp$ -space) devoid of any impurities is, up to pre-exponential factors, given by

$$w \sim \exp(-c L_R^{d_\perp}) : \quad (4)$$

As discussed in Sec. 2, such a rare region develops static long-range order at some  $t_c(L_R)$  below the clean critical point  $t_c^0 = 0$ . The value of  $t_c(L_R)$  varies with the size of the region: The largest islands develop long-range order closest to the clean

<sup>z</sup> Note that global thermodynamic variables (which average over the entire sample) do not resolve the strong spatial inhomogeneities which are the hallmark of a smeared transition, and thus do not provide complete information about the transition

<sup>x</sup> We use the bare value,  $t_c^0 = 0$ , for the clean critical reduced temperature. For our purpose, the distinction between the bare and the renormalized  $t$  is of no importance.

critical point. Finite size scaling (for the clean system, because the island is devoid of impurities) yields

$$t_c^0 - t_c(L_R) = j_c(L_R)j = A L_R^{-\nu} \quad (5)$$

where  $\nu$  is the finite-size scaling shift exponent and  $A$  is the amplitude for the crossover from  $d$  dimensions to a slab geometry in finite in two dimensions but finite in  $d_2 = d - 2$  dimensions. Combining (4) and (5) we obtain the probability for finding a rare region which becomes critical at  $t_c$  as

$$w(t_c) = \exp(-B j^{-d_2}) \quad (\text{for } t \neq 0) \quad (6)$$

where the constant  $B$  is given by  $B = cA^{d_2}$ . The total (or average) order parameter  $m$  is obtained by integrating over all rare regions which are ordered at  $t$ , i.e., all rare regions having  $t_c > t$ . Since the functional dependence on  $t$  of the order parameter on a given island is of power-law type it does not enter the leading exponentials but only the pre-exponential factors. Therefore we obtain to exponential accuracy

$$m = \exp(-B j^{-d_2}) \quad (\text{for } t \neq 0) : \quad (7)$$

The homogeneous magnetic susceptibility consists of two different contributions, one from the islands on the verge of ordering and one from the bulk system still deep in the disordered phase. The bulk system provides a finite, noncritical background susceptibility throughout the tail region of the smeared transition. In order to estimate the contribution of the islands consider the onset of local ordering at the clean critical temperature  $t_c^0 = 0$ . Using (6) for the density of the islands we can estimate

$$\int_0^\infty dt t^{-\nu} \exp(-B t^{-d_2}) \quad (8)$$

which is finite because the exponentially decreasing island density overcomes the power-law divergence of the susceptibility of an individual island. Here  $\nu$  is the clean susceptibility exponent and  $\nu$  is related to a lower cutoff for the island size. Once ordered islands exist they produce an effective background magnetic field everywhere in space which cuts off any possible divergence. Therefore we conclude that the homogeneous magnetic susceptibility does not diverge anywhere in the tail region of the smeared transition. However, there is an essential singularity at the clean critical point produced by the vanishing density of ordered islands.

The spatial magnetization distribution in the tail of the smeared transition is very inhomogeneous. On the already ordered islands, the local order parameter  $m(r)$  is of the same order of magnitude as in the clean system. Away from these islands it decays exponentially with the distance from the nearest island. The probability distribution  $P[\log m(r)]$  will therefore be very broad, ranging from  $\log m(r) = 0$  (1) on the largest islands to  $\log m(r) \rightarrow -\infty$  on sites very far away from an ordered island. The typical local order parameter  $m_{\text{typ}}$  can be estimated from the typical distance of any point to the nearest ordered island. From (6) we obtain

$$r_{\text{typ}} = \exp(B j^{-d_2}) : \quad (9)$$

At this distance from an ordered island, the local order parameter has decayed to

$$m_{\text{typ}} = e^{-r_{\text{typ}}/\xi_0} = \exp(-C \exp(B j^{-d_2})) \quad (10)$$

where  $\xi_0$  is the bulk correlation length (which is finite and changes slowly throughout the tail region of the smeared transition) and  $C$  is constant. A comparison with (7) gives the relation between  $m_{\text{typ}}$  and the thermodynamic order parameter,

$$j \log m_{\text{typ}} j = m^{-1/d_2} : \quad (11)$$

Thus,  $m_{\text{typ}}$  decays exponentially with  $m$  indicating an extremely broad local order parameter distribution. In order to determine the functional form of the local order parameter distribution, first consider a situation with just a single ordered island at the origin of the coordinate system. For large distances  $r$  the magnetization falls off exponentially like  $m(r) = m_0 e^{-r/\xi_0}$ . The probability distribution of  $x = \log[m(r)] = \log m_0 - r/\xi_0$  can be calculated from

$$P(x) = \frac{dN}{dx} = \frac{dN}{dr} \frac{dr}{dx} = \xi_0 \frac{dN}{dr} e^{-x/\xi_0} \quad (12)$$

where  $dN$  is the number of sites at a distance from the origin between  $r$  and  $r + dr$  or, equivalently, having a logarithm of the local magnetization between  $x$  and  $x + dx$ . For large distances we have  $x \approx -r/\xi_0$ . Therefore, the probability distribution of  $\log m$  generated by a single ordered island takes the form

$$P[\log(m)] = j \log(m)^{j-1} \quad (\text{form 1}) : \quad (13)$$

In the tail region of the smeared transition the system consists of a few ordered islands whose distance is large compared to  $\xi_0$ . The probability distribution of  $\log[m(r)]$  thus takes the form (13) with a lower cutoff corresponding to the typical island-island distance and an upper cutoff corresponding to a distance  $\xi_0$  from an ordered island.

### 3.2. Finite-size effects

It is important to distinguish effects of a finite size  $L_C$  in the correlated directions and a finite size  $L_\perp$  in the uncorrelated directions. If  $L_\perp$  is finite but  $L_C$  is infinite static order on the rare regions can still develop. In this case, the sample contains only a finite number of islands of a certain size. As long as the number of relevant islands is large, finite size-effects are governed by the central limit theorem. However, for  $t \rightarrow 0$  very large and rare islands are responsible for the order parameter. The number  $N$  of islands which order at  $t_c$  behaves like  $N \sim L_\perp^{d_\perp} w(t_c)$ . When  $N$  becomes of order one, strong sample-to-sample fluctuations arise. Using (6) for  $w(t_c)$  we find that strong sample to sample fluctuations start at

$$j_{L_\perp} = j + \frac{d_\perp}{B} \log(L_\perp) : \quad (14)$$

Thus, finite size effects are suppressed only logarithmically.

Analogously, one can study the onset of static order in a sample of finite size  $L_\perp$  (i.e., the ordering temperature of the largest rare region in this sample). For small sample size  $L_\perp$ , the probability distribution  $P(t_c)$  of the sample ordering temperatures  $t_c$  will be broad because some samples do not contain any large islands. With increasing sample size the distribution becomes narrower and moves towards the clean  $t_c^0$  because more samples contain large islands. The maximum  $t_c$  coincides with  $t_c^0$  corresponding to a sample without impurities. The lower cutoff corresponds to an island size so small that essentially every sample contains at least one of them. Consequently, the width of the distribution of critical temperatures in finite-size samples is governed by the same relation as the onset of the fluctuations,

$$t_c = t_c^0 + \frac{d_\perp}{B} \log(L_\perp) : \quad (15)$$

We now turn to finite-size effects produced by a finite extension  $L_C$  of the system in the correlated directions. In this case, the true static order on the rare regions

is destroyed. Whether or not the system develops long-range order depends on the number  $d_2$  of uncorrelated dimensions. If  $d_2 = 1$  no static long-range order can develop, i.e. the transition is rounded by conventional finite size effects in addition to the disorder-induced smearing. In contrast, for  $d_2 > 1$  a true phase transition is possible but requires a finite interaction between the islands of the order of the temperature. This restores a sharp phase transition at a reduced temperature  $t_c(L_C)$ . To estimate the relation between  $L_C$  and  $t_c(L_C)$  we note that the interaction between two planar rare regions of linear size  $L_C$  is proportional to  $L_C^2$  and decays exponentially with their spatial distance  $r$ ,  $E_{int} \sim L_C^2 \exp(-r/\xi_0)$ , where  $\xi_0$  is the bulk correlation length. With the typical distance given by (9) we obtain a double exponential dependence between  $L_C$  and the critical reduced temperature  $t_c(L_C)$ :

$$\log(\log L_C) \sim \frac{1}{d_2} : \quad (16)$$

### 3.3. Gaussian disorder

In this subsection we apply Lifshitz tail arguments to the case of  $\delta$ -correlated Gaussian disorder [34]. In contrast to the positive definite Poisson disorder, the Gaussian disorder is unbounded for  $t(r) \rightarrow 1$ . Therefore, locally ordered islands can exist for all  $t$ , and, in principle, the tail region of the smeared transition stretches to  $t \rightarrow 1$ . In order to determine the probability for finding a rare region which orders at a certain  $t_c$ , i.e., the Gaussian equivalent to (6), consider an island of linear size  $L_R$ . The average disorder value  $h$  in this region has the distribution

$$P[h] \sim \exp(-L_R^{d_2} h^2) : \quad (17)$$

According to finite size scaling, an island of size  $L_R$  with an average disorder value of  $h$  will develop static order at  $t_c = h t_c^0 A L_R$ . For fixed island size, the probability distribution of  $t_c$  reads

$$P(t_c) \sim \exp(-L_R^{d_2} (t_c + A L_R)^2) : \quad (18)$$

We now calculate the stationary point of the exponent with respect to  $L_R$  (saddle point approximation) to determine which island size gives the dominating contribution. For  $(2 - d_2) > 0$ , this leads to

$$(2 - d_2) A L_R = t_c d_2 : \quad (19)$$

This implies that small but very deep fluctuations are responsible for the tail of the smeared transition (in contrast to Poisson disorder where the tail is produced by the largest islands). Inserting into (18) gives the desired probability as a function of  $t_c$ ,

$$w(t_c) \sim \exp(-B t_c^{2-d_2}) \quad (20)$$

where  $B$  is a constant. In contrast, for  $(2 - d_2) < 0$ , the main contribution comes from arbitrarily small islands. In this case the  $\delta$ -correlated disorder is unphysical and should be replaced by a distribution with a finite correlation length. The resulting  $w(t_c)$  is then purely Gaussian. In the following we will not consider this case.

Starting from (20), one can derive the leading behavior in the tail of the smeared transition ( $t \rightarrow 1$ ). Integrating over all ordered islands gives the total magnetization

$$m \sim \exp(-B t_c^{2-d_2}) : \quad (21)$$

The typical local magnetization  $m_{typ}$  decays exponentially with the average magnetization  $m$ , i.e. (11) also holds in the Gaussian case as can be easily seen by

starting the derivation from (20) rather than (6). For samples of finite size in the uncorrelated directions the onset of sample-to-sample fluctuations and the width of the sample ordering temperatures follow

$$t_{L_2} - t_c \sim (\log L_2)^{1/(2-d_2)} : \quad (22)$$

If the samples are of finite size in the correlated directions but infinite in the uncorrelated ones (and if  $d_2 > 1$ ) a sharp phase transition is restored. The relation between  $L_C$  and  $t_c$  is double-exponential:

$$\log(\log L_C) \sim \frac{2}{d_2 - 1} : \quad (23)$$

A comparison of the results for Gaussian and Poisson disorder shows that the functional form of the thermodynamic relations at the smeared transition depends on the form of the disorder and is thus not universal.

#### 4. Numerical results

##### 4.1. Model and method

To illustrate the smearing of the phase transition we now show results from a numerical simulation of a 3D Ising model with planar bond defects, i.e.,  $d_c = 2$  and  $d_2 = 1$ . As discussed above, the smearing of the phase transition is the result of exponentially rare events. Therefore large system sizes are required to observe it. In order to reach sufficiently large sizes with a reasonable effort and to retain the possibility of static order on an isolated rare region, we consider a model with infinite-range interactions in the correlated directions (parallel to the defects) but short-range interactions in the uncorrelated direction (perpendicular to the defect planes). While the infinite-range model will not be quantitatively comparable to a short-range model, it provides a simple example for the rounding mechanism introduced in Sec. 2. Moreover, since the rounding mechanism only depends on the existence of static order on the rare regions but not on any details, we expect that the results will be qualitatively valid for a short-range model, too (with the appropriate changes to the exponents in the relations derived in Sec. 3). Indeed, preliminary results [35] of Monte-Carlo simulations of a 3D short-range Ising model with planar defects fully agree with this expectation.

The Hamiltonian considered in this section reads

$$H = \frac{1}{L_C^2} \sum_{x,y,z;y^0;z^0} S_{x,y,z} S_{x+1,y^0,z^0} - \frac{1}{2L_C^2} \sum_{x,y,z;y^0;z^0} J_x S_{x,y,z} S_{x,y^0,z^0} - h \sum_{x,y,z} S_{x,y,z} : (24)$$

Here  $x,y,z$  are the integer-valued coordinates of the Ising spins. The magnetic field  $h$  acts as a symmetry breaker, it will be set to a small but non-zero value, typically  $h = 10^{-10}$ .  $L_C$  is the system size in the  $y$  and  $z$  directions. The planar defects are parallel to the  $(y,z)$ -plane. They are introduced via disorder in the in-plane coupling  $J_x$  which is a quenched binary random variable with the distribution  $P(J) = (1-c)\delta(J-1) + c\delta(J-J_d)$  with  $J_d < 1$ . Here,  $c$  is the defect concentration and the deviation of  $J_d$  from 1 measures the strength of the defects. For our calculations we use  $J_d = 0$ , i.e., very strong defects. The fact that one can independently vary concentration and strength of the defects in an easy way is the main advantage of this binary disorder distribution. However, it also has unwanted consequences, viz. log-periodic oscillations of many observables as functions of the distance from the critical point [36]. These oscillations are special to the binary distribution and unrelated to the smearing considered here; we will not discuss them further.



Because the interaction is infinite-ranged in the correlated ( $y$  and  $z$ ) directions, these dimensions can be treated exactly: We introduce the plane magnetizations

$$m_x = \frac{1}{L_C^2} \sum_{y,z} S_{x,y,z} \quad (25)$$

into the partition function and integrate out the original Ising variables  $S_{x,y,z}$ . In the thermodynamic limit,  $L_C \rightarrow \infty$ , the resulting integral can be solved using saddle point approximation. This leads to a set of coupled local mean-field equations

$$m_x = \tanh [(m_{x-1} + J_x m_x + m_{x+1} + h)/T] ; \quad (26)$$

where  $T$  is the temperature (we work in units where the Boltzmann constant is  $k_B = 1$ ). In the clean case,  $c = 0$ , all  $J_x$  are equal to 1. Consequently, all local mean-field equations are identical, reading  $m = \tanh [(3m + h)/T]$ . The clean critical temperature of the model (24) is therefore  $T_c^0 = 3$ .

In the presence of disorder, the local mean-field equations (26) have to be solved numerically. We employ a simple self-consistency cycle: All  $m_x$  are initially set to  $m_x = 0.1$ . We then insert the current values of  $m_x$  into the r.h.s. of (26) and calculate new values  $m_x^{\text{new}}$  which are then put into the r.h.s. and so on. This is repeated until the change  $\sum_x |m_x^{\text{new}} - m_x|$  falls below a threshold of  $10^{-12}$  for all  $x$ . This method is very robust, it never failed to converge, but it can be very slow in the tail region of the transition where ordered islands coexist with large disordered regions. In this region sometimes several 1000 iterations were necessary. However, in contrast to more sophisticated methods like the Newton-Raphson method no matrix inversions are required. Therefore we were able to simulate very large systems up to  $L_z = 10^6$ .

We also note that the model (24) is similar to the mean-field McCoy-Wu model considered in Ref. [37]. The raw data obtained in this paper ( $L_z$  up to 1000) are very similar to ours, but they were interpreted in terms of conventional power-law critical behavior with an unusually large order parameter exponent  $3.6$ . This may be partially due to an unfortunate choice of parameters (in particular, a higher impurity concentration of  $c = 0.5$ ) which makes it harder to observe the exponential tail of the smeared transition. We will come back to this question in Sec. 5.

#### 4.2. Thermodynamic magnetization and susceptibility

In this subsection we present numerical results for the total magnetization  $m = L_z^{-1} \sum_x m_x$  and the homogeneous susceptibility  $\chi = \partial m / \partial h$ . The left panel of figure 1 gives an overview over the behavior of  $m$  and  $\chi$  as functions of temperature  $T$  for size  $L_z = 1000$  and impurity concentration  $c = 0.2$ . The data are averages over 1000 disorder realizations. (Thermodynamic quantities involve averaging over the whole system. Thus ensemble averages rather than typical values give the correct infinite system approximation.) At a first glance these data suggest a sharp phase transition close to  $T = 2.96$ . However, a closer inspection of the transition region in the right panel of figure 1 shows that the singularities are rounded. If this smearing was a conventional finite-size effect the magnetization curve should become sharper with increasing  $L_z$  and the susceptibility peak should diverge. This is not the case here, both the magnetization and the susceptibility data are essentially size-independent. We conclude that the smearing is an intrinsic effect of the infinite system.

In order to compare the total magnetization data with the analytical Lifshitz tail prediction (7) we need to determine the value of the clean finite-size scaling shift

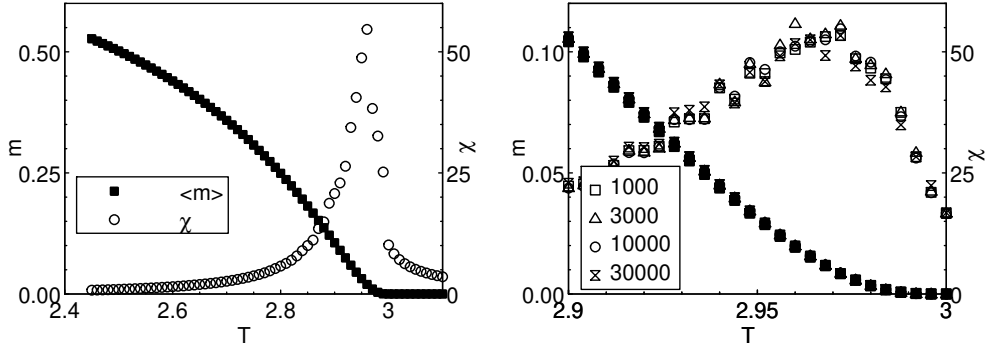


Figure 1. Left: Magnetization  $m$  and susceptibility  $\chi$  for  $L_z = 1000$ ;  $c = 0.2$ . Right: Magnetization and susceptibility close to the seeming transition for different system sizes  $L_z$  in the uncorrelated direction.

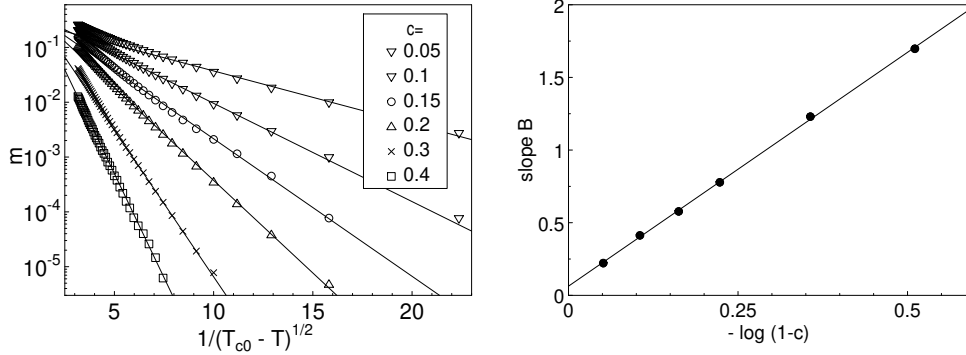


Figure 2. Left: Total magnetization  $m$  as a function of  $(T_c^0 - T)^{-1/2}$  for several impurity concentrations  $c$ . The solid lines are fits to eq. (7) with  $\beta = 2$ . Right: Decay constant  $B$  as a function of  $-\log(1-c)$ .

exponent for them model (24). Finite-size scaling is governed by the first appearance of a non-vanishing solution of the linearized clean mean-field equation in a slab geometry of varying thickness. This equation is equivalent to a one-dimensional Schrödinger equation in a potential well, leading to a clean shift exponent of  $\beta = 2$  and  $d_\beta = 1/2$ . In the left panel of figure 2, we therefore plot the logarithm of the total magnetization, averaged over 300 samples, as a function of  $(T_c^0 - T)^{-1/2}$  for system size  $L_z = 10000$  and several impurity concentrations  $c$ . For all  $c$ , the data follow eq. (7) over several orders of magnitude in  $m$ . Fits of the data to (7) are used to determine the decay constants  $B$ . The right panel of figure 2 shows that these decay constants depend linearly on  $-\log(1-c)$ . This is exactly the expected behavior in a lattice model with binary disorder since the probability for finding an island of size  $L_R$  devoid of impurities behaves like  $(1-c)^{L_R} \approx e^{-L_R \log(1-c)}$ .

#### 4.3. Local magnetization

In the tail region of the smeared transition the system consists of a few rare ordered regions (on sufficiently large islands devoid of impurities). These rare regions are far apart, and between them the local magnetization is exponentially small. This behavior

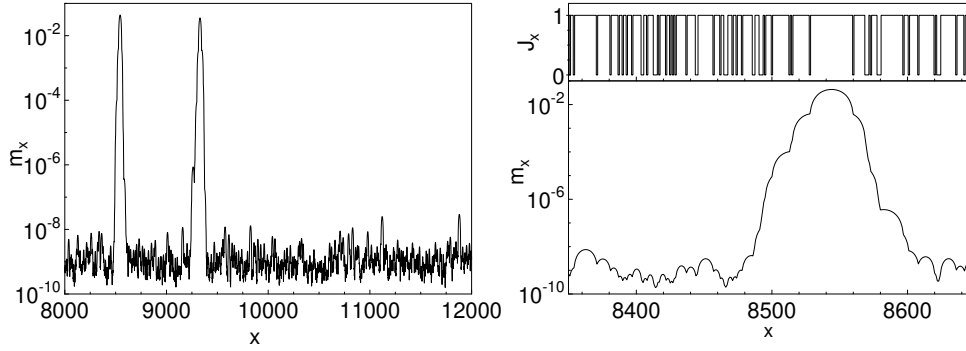


Figure 3. Left: Local magnetization  $m_x$  vs.  $x$  for a segment of a single sample with size  $L_\perp = 100000$ , impurity concentration  $c = 0.2$  and temperature  $T = 2.99$ . Right: Local magnetization  $m_x$  and local coupling constant  $J_x$  in the vicinity of one of the ordered islands.

is illustrated in figure 3. The left panel shows the local magnetization of a segment of a large sample in the tail region of the smeared transition. The data show that the local magnetization on the islands is large ( $\approx 0.1$ ) but it drops very rapidly with increasing distance from the islands. This drop-off can be used to estimate the bulk correlation length which is very small in this parameter region,  $\xi_0 \approx 3 \div 4$ . Note that the seeming saturation of the magnetization decrease at  $m \approx 10^{-9}$  is a result of the finite external field  $h = 10^{-10}$ . Without field, the magnetization would drop much further. A comparison of the local magnetization  $m_x$  and the local coupling constant  $J_x$  in the right panel of figure 3 shows that magnetic order only exists on a sufficiently large island devoid of any impurities.

In order to quantify these observations, we have also calculated the probability distribution  $P(\log m_x)$  of the local magnetization values, or, more precisely, their logarithms. Figure 4 shows this distribution for a single large sample of  $L_\perp = 200000$ , impurity concentration  $c = 0.2$ , and temperatures ranging from  $T = 2.8$  (deep in the ordered phase) to  $T = 2.99$  (in the tail of the smeared transition). Clearly, with increasing temperatures the distribution becomes very broad, even on this logarithmic scale. Two qualitatively different regimes can be distinguished. For temperatures not too close to the clean critical point ( $T = 2.80$  to  $2.96$ ), the distribution is dominated by an exponential decay towards small magnetization values (i.e., towards negative  $\log m$ ) with the decay constant decreasing with increasing temperature. However, once the system enters the rare-region dominated tail region of the smeared transition (which, as can be seen from figures 1 and 2, happens roughly at  $T = 2.96 \div 2.97$  for  $c = 0.2$ ) the behavior changes: In agreement with (13) the probability distribution  $P(\log m_x)$  becomes constant except for a peak at large magnetization values which we attribute to the behavior of  $m_x$  on the ordered islands (eq. (13) was derived from the behavior of the sites not belonging to one of the rare ordered islands).

#### 4.4. Finite-size effects and sample-to-sample fluctuations

In this subsection we present numerical data for the effects of a finite sample size  $L_\perp$  in the uncorrelated direction, i.e., perpendicular to the impurities. Effects of a finite size  $L_C$  in the correlated directions cannot easily be studied within our approach because

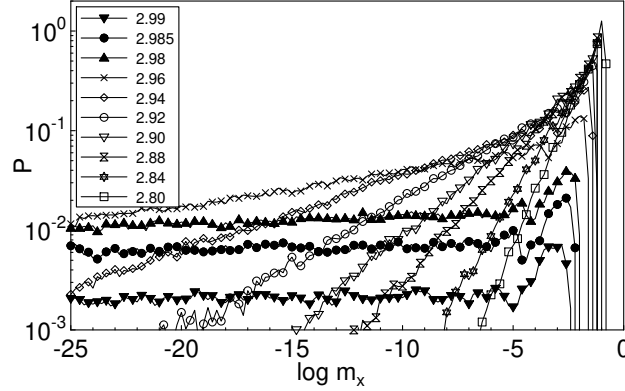


Figure 4. Probability distribution of the local magnetization  $m_x$  for single sample of size  $L_2 = 200000$ , impurity concentration  $c = 0.2$  and several temperatures. The three curves represented by filled symbols ( $T = 2.98$ ) are in the asymptotic regime described by eq. (13).

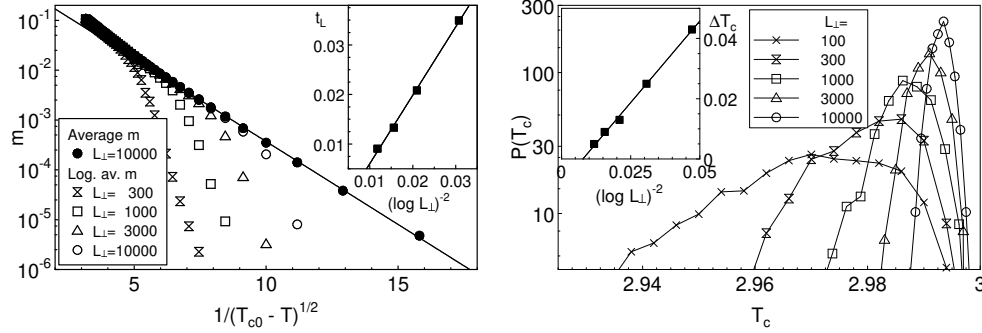


Figure 5. Left: Average and typical (log. averaged) sample magnetization for  $c = 0.2$  and different sample sizes. The inset shows the onset temperature of strong sample-to-sample fluctuations (measured by  $t_L = T_c^0 - T_L$ ) as a function of  $(\log L_2)^{-2}$ . Right: Probability distribution of the sample ordering temperatures for  $c = 0.2$  and different sample sizes. The inset shows the width  $\Delta T_c$  of this distribution as a function of  $(\log L_2)^{-2}$ .

the limit  $L_C \rightarrow 1$  has been taken in deriving the local mean-field equations (26).

To investigate sample-to-sample fluctuations in a finite-size system we compare the average sample magnetization  $m_{av} = \langle m \rangle$  and the typical sample magnetization  $m_{typ} = \exp(\log m)$  where  $m$  is the total magnetization of a sample and  $\langle \cdot \rangle$  denotes the average over the disorder. A significant difference between average and typical magnetizations indicates strong sample-to-sample fluctuations. The left panel of figure 5 shows the typical magnetizations for four different sizes  $L_2$  together with the average magnetization (which is size-independent within the accuracy of this plot) for 300 to 1000 samples, depending on  $L_2$ . In the tail region of the smeared transition the typical and average magnetizations deviate from each other by several orders of magnitude. From these data we define a temperature  $T_{L_2}$  which describes the onset of the sample-to-sample fluctuations via  $m_{av}(T_{L_2}) = m_{typ}(T_{L_2}) = e$ . This temperature shifts to larger values with increasing system size  $L_2$ . The inset shows  $t_{L_2} = T_c^0 - T_{L_2}$  as a function

of  $(\log L_\perp)^{-2}$ . The plot shows that  $t_{L_\perp}$  follows eq. (14) in good approximation.

The right panel of figure 5 shows the probability distribution of the sample critical temperature which is defined as the ordering temperature of the largest rare region in a particular sample (600 to 2000 samples used). As predicted in subsection 3.2, the distribution becomes narrower with increasing size  $L_\perp$ , and it shifts towards the clean critical temperature  $T_c^0 = 3$ . The width  $\Delta T_c$  of this distribution has been determined from the values where  $P$  has decreased by a factor of  $1/e$ . The inset shows that  $\Delta T_c$  is proportional to  $(\log L_\perp)^{-2}$  as predicted in eq. (15).

## 5. Discussion

To summarize, we have shown that true static order can develop on an isolated rare region in an Ising model with planar defects. As a result, different parts of the system undergo the phase transition at different temperatures, i.e., the sharp transition is smeared by the defects. In this final section we discuss the generality of our findings and their relation to Griffiths phenomena and the Harris criterion. We also discuss favorable conditions for observing the smearing in experiments or simulations.

The origins of the smearing of the phase transition introduced in this paper and of Griffiths phenomena are very similar, both are caused by rare large spatial regions which are locally in the ordered phase. The difference between the two effects is a result of disorder correlations. For uncorrelated or short-range correlated disorder, the rare regions are of finite size. Thus, they cannot develop true static long-range order. Instead, the order parameter fluctuates slowly leading to the Griffiths singularities [6] discussed in Sec. 1. In contrast, if the rare regions are infinite in at least two dimensions, a stronger effect occurs: the rare regions which are locally in the ordered phase actually develop true static order, and this leads to a smeared transition. In other words, the same rare regions which would usually produce Griffiths singularities are responsible for the smearing of the transition in a system with planar defects. The tail of the smeared transition stretches to where the Griffiths temperature would normally be, i.e., to  $T = 1$  for Gaussian disorder or  $T = T_c^0$  for Poisson disorder. So, the smeared transition replaces not only the conventional critical point but also the Griffiths phase.

We now discuss under which conditions a phase transition will be smeared by disorder. The arguments given in Sec. 2 in favor of a smeared transition only relied on the dimensionality of the rare regions and the order parameter symmetry. It is therefore expected that all phase transitions with discrete order parameter symmetry are smeared by quenched disorder if the defects are perfectly correlated in at least two dimensions. In systems with linear defects the transition will remain sharp if the interactions are short-ranged. However, if the interactions in the correlated direction fall off as  $1=r^{-2}$  or slower, even linear defects can lead to smearing because a 1D Ising model with  $1=r^{-2}$  interaction has an ordered phase [38]. This is particularly important [39] for quantum phase transitions in itinerant electronic systems which can be mapped onto classical systems with  $1=r^{-2}$  interaction in imaginary time direction.

Phase transitions with continuous order parameter symmetry are more stable against smearing. In systems with short-range interactions the dimensionality of the defects has to be at least three, and in systems with linear or planar defects long-range interactions are required for smearing. It is known [40] that classical XY and Heisenberg systems in dimensions  $d = 1; 2$  develop long-range order at finite  $T$  only if the interaction falls off more slowly than  $1=r^{2d}$ . Consequently, in a system with linear

defects the phase transition will only be smeared if the interactions in defect direction fall off more slowly than  $1=r^{-2}$  (or more slowly than  $1=r^4$  for planar defects).

A third important question concerns the universality of the thermodynamic behavior in the vicinity of the smeared transition. As can be seen from comparing the results of Poisson and Gaussian disorder, the functional dependence of the magnetization and other observables on the temperature is not universal, it depends on details of the disorder distribution. Therefore, only the presence or absence of smearing is universal in the sense of critical phenomena (i.e., depending on dimensionality and symmetry only) while the thermodynamic relations are non-universal.

Our fourth remark deals with the relation of the disorder-induced smearing and the Harris criterion which in the case of extended defects reads  $[21] \quad \nu > 2/d$ . We emphasize that the phase transition can be smeared by planar defects even if the corresponding clean critical point fulfills the Harris criterion and appears to be stable. The reason is that the Harris criterion assumes a homogeneous transition and studies the behavior of the coarse-grained (root-mean-square) disorder at large length scales. However, the formation of static order on an isolated finite-size rare region is a non-perturbative finite-length scale effect in the tail of the disorder distribution. This type of effects is not covered by the Harris criterion.

We now turn to the question which conditions are favorable for the observation of the smearing in experiments or simulations. A significant number of large rare regions will only exist if the defect concentration is small, as can be seen from (6). On the other hand, the impurities have to be sufficiently strong so that the bulk system is still far away from criticality when the first rare regions start to order. Thus, the most favorable type of disorder for the observation of the smearing is a small density of strong impurities. In contrast, for weak impurities the rounding is restricted to a very narrow temperature range below the clean critical temperature and maybe masked by the remainder of the bulk critical fluctuations. If the impurity concentration is too high, the exponential drop-off is very fast making it very hard to observe the smearing. This may also explain why no smearing was observed in earlier simulations. Specifically, in Ref. [23] weak impurities ( $J=J_0=0.1$ ) of a high concentration  $c=0.5$  were used. These are unfavorable conditions, and the maximum system size of  $L=27$  used in this simulation was probably too small to observe the smearing.

Finally, we add one remark about the extreme tail of the smeared transition. In this parameter region, the ordered islands are very far apart and the aligning effect of the direct island-island interactions is very weak. It is therefore possible that in a real system other interactions play an important role in determining the relative orientation of the order parameter on the islands. This could lead, e.g., to spin glass order in the extreme tail of the smeared transition.

In conclusion, perfect disorder correlations in one or more directions dramatically increase the effects of the disorder on a phase transition with discrete order parameter symmetry. Zero-dimensional defects typically lead to a conventional critical point with power-law scaling. For linear defects the generic behavior seems to be an infinite-randomness critical point [24,25,28] while we have shown here that planar defects generically destroy the sharp transition by smearing.

Acknowledgments

We acknowledge support from the University of Missouri Research Board. Part of this work has been performed at the Aspen Center for Physics.

## References

- [1] Grinstein G 1985 Fundamental Problems in Statistical Mechanics VI, ed E G D Cohen (New York Elsevier) p.147
- [2] Harris A B 1974 J. Phys. C 7 1671
- [3] Aharony A and Harris A B 1996 Phys. Rev. Lett. 77 3700
- [4] Wiseman S and Domany E 1998 Phys. Rev. Lett. 81 22
- [5] McCoy B M and Wu T T 1968 Phys. Rev. 176 631
- [6] McCoy B M and Wu T T 1969 Phys. Rev. 188 982
- [7] Griffiths R B 1969 Phys. Rev. Lett. 23 17
- [8] Randeria M, Sethna J, and Palmer R G 1985 Phys. Rev. Lett. 54 1321
- [9] Bray A J and Huifang D 1989 Phys. Rev. B 40 6980
- [10] Dhar D 1983 Stochastic Processes: Formalism and Applications, ed D S Argywal and S Dattagupta (Berlin Springer)
- [11] Dhar D, Randeria M, and Sethna J P 1988 Europhys. Lett. 5 485
- [12] Bray A J 1988 Phys. Rev. Lett. 60 720
- [13] Bray A J and Rodgers G J 1988 Phys. Rev. B 38 9252
- [14] Bray A J 1987 Phys. Rev. Lett. 59 586
- [15] Dreyfus H von, Klein A, and Perez J F 1995 Commun. Math. Phys. 170 21
- [16] Gielis G and Maes C 1995 J. Stat. Phys. 81 829
- [17] Cesi S, Maes C, and Martinelli F 1997 Commun. Math. Phys. 189 135
- [18] Cesi S, Maes C, and Martinelli F 1997 Commun. Math. Phys. 189 323
- [19] Lubensky T C 1975 Phys. Rev. B 11 3573
- [20] Rudnick J 1978 Phys. Rev. B 18 1406
- [21] Andelman D and Aharony A 1985 Phys. Rev. B 31 4305
- [22] Dorogovtsev S N 1980 Fiz. Tverd. Tela (Leningrad) 22 321 [Sov. Phys. (Solid State 22 188)]
- [23] Boyanovsky D and Cardy J L 1982 Phys. Rev. B 26 154
- [24] De Cesare L 1994 Phys. Rev. B 49 11742
- [25] Lee J C and Gibbs R L 1992 Phys. Rev. B 45 2217
- [26] McCoy B M 1969 Phys. Rev. Lett. 23 383
- [27] Fisher D S 1992 Phys. Rev. Lett. 69 534
- [28] Fisher D S 1995 Phys. Rev. B 51 6411
- [29] Young A P and Rieger H 1996 Phys. Rev. B 53 8486
- [30] Pich C, Young A P, Rieger H, and Kawashima N 1998 Phys. Rev. Lett. 81 5916
- [31] Motrunich O, Ma S-C, Huse D A, and Fisher D S 2000 Phys. Rev. B 61 1160
- [32] Ma S K, Dasgupta C, and Hu C-K 1979 Phys. Rev. Lett. 43 1434
- [33] Bhatt R N and Lee P A 1982 Phys. Rev. Lett. 48 344
- [34] Fisher D S 1994 Phys. Rev. B 50 3799
- [35] Huse D A private communication
- [36] Lifshitz I M 1964 Usp. Fiz. Nauk 83 617 [Sov. Phys. (Usp. 7 549)]
- [37] Friedberg R and Luttinger J M 1975 Phys. Rev. B 12 4460
- [38] Halperin B I and Lax M 1966 Phys. Rev. 148 722
- [39] Sknepnek R and Vojta T unpublished
- [40] Karevski D and Turban L 1996 J. Phys. A 29 3461
- [41] Berche B, Berche P E, Igloi F, and Palagyi G 1998 J. Phys. A 31 5193
- [42] Thouless D J 1969 Phys. Rev. 187 732
- [43] Cardy J 1981 J. Phys. A 14 1407
- [44] Vojta T 2003 Phys. Rev. Lett. 90 107202
- [45] Bruno P 2001 Phys. Rev. Lett. 87 137203